

# Studying Soft Gluon Radiation in $t\bar{t}$ events at a Linear Collider

Steve Vejcik  
Fermi National Accelerator Laboratory

## 1 Introduction

The production and decay of top quarks provides an interesting configuration of, and interplay between, color fields whose transience limits their interactions to the emission of soft gluons. Because of the large top mass ( $M_t \approx 175 \text{ GeV}/c^2$ ), gluon production coupled to the top colored charge exhibits different kinematic properties compared with other colored objects. Because of the large value of the electroweak decay width ( $\Gamma_t \approx 1.5 \text{ GeV}$ ), emissions from the top quark can be suppressed by interference with those from the  $b$ -quark produced in the top quark's electroweak decay. This offers the possibility of extracting the top quark lifetime through measurement of properties associated with soft gluon emissions. It is argued here that studies of hadroproduction in  $t\bar{t}$  events produced from  $e^+e^-$  collisions, in particular, offers an experimentally feasible means of measuring  $\Gamma_t$  and radiation patterns produced by a massive colored object. After reviewing basic features of top production for scenarios involving linear  $e^+e^-$  colliders, there will follow a review of different descriptions of shower and hadron production, focusing on those elements that are distinctive for  $t\bar{t}$  production. Finally, a set of schema for experimental measurements and an estimate of the precision with which  $\Gamma_t$  might be measured are described in the last section.

## 2 Top Production at Linear Colliders

Many elements of a program for the study of top quarks at a high energy linear  $e^+e^-$  collider have been discussed extensively elsewhere [?]. Particularly important operation is at the  $t\bar{t}$  threshold,  $\sqrt{s} \approx 350 \text{ GeV}$ , where the measurement of the inclusive cross section yields precise measurements of both  $M_t$  and  $\Gamma_t$ . Another commonly discussed sce-

nario is operation at  $\sqrt{s} = 500 \text{ GeV}$  where production rates for  $t\bar{t}$  are still high. This is the scenario considered here. At design luminosities [?], one year of running at this energy would allow the delivery of an integrated luminosity of  $100 - 300 \text{ fb}^{-1}$ . With a cross section for  $e^+e^- \rightarrow t\bar{t}$  of  $650 \text{ fb}$  [?], accumulated samples of 65,000-200,000  $t\bar{t}$  would be available in 1-2 years of running. As opposed to a hadronic machine, it will be very straightforward to collect these events with high efficiency. For the purposes of this study, it is assumed that events of the type  $e^+e^- \rightarrow t\bar{t} \rightarrow W^+bW^-\bar{b}$  followed by the leptonic decay of one or both of the  $W$  bosons will be well measured through the reconstruction of high momentum jets, missing energy, and one or two leptons ( $e$  or  $\mu$ ). Events with one leptonic decay, also referred to as Lepton+Jet events, have a branching ratio of  $24/81 \approx 0.30$  while dilepton events have a branching ratio of  $4/81 \approx 0.05$ .

## 3 QCD and Soft Gluon Production from Massive Objects

### 3.1 Eikonal Description

Much of the interesting physics pertaining to soft gluon production from massive objects can be understood in the context of the eikonal treatment. For the particular case of top quark production, a detailed treatment can be found in Reference [?]. The main result is the calculation of the cross section for the production of a single gluon from the color structure produced in  $e^+e^- \rightarrow t\bar{t} \rightarrow WbW\bar{b}$  events expressed as a linear sum of antennae:

$$\frac{d\sigma}{\sigma} = \sum_i c(\Gamma_t)_i \hat{p}_i \hat{q}_i \quad (1)$$

The antennae are analytic functions of the four momenta of the partons involved in the problem.

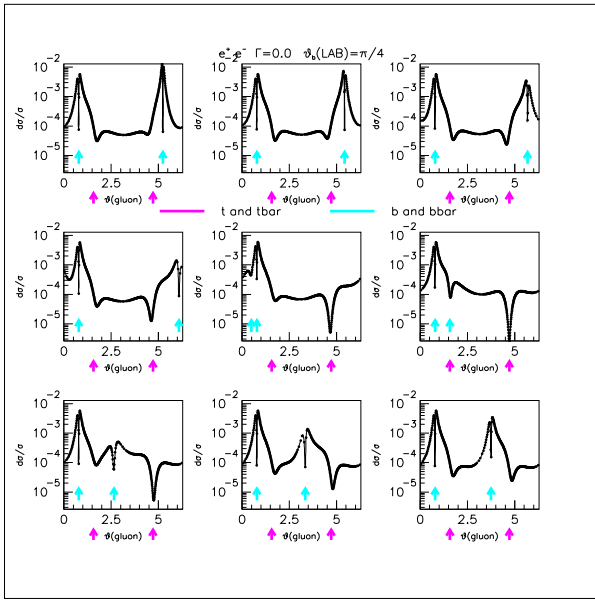


Figure 1: Radiation patterns calculated by eikonal description with the top width,  $\Gamma_t$ , set to 0. Each plot shows the single gluon production differential cross section (normalized to the hard scattering Born cross section) *vs* the polar angle  $\theta$ . Confined to two dimensions,  $0 < \theta < 2\pi$ .

Figure 1 shows examples of radiation patterns for different kinematic configurations of the  $t$ ,  $\bar{t}$ ,  $b$ , and  $\bar{b}$  quarks, and illustrates most of the salient features of soft gluon emission.

Each radiation pattern displays the differential gluon emission cross section,  $\frac{1}{\sigma_0} \frac{d\sigma}{d\theta}$ , plotted *vs*  $\theta$  where  $\theta$  is polar angle of the gluon. For the cases shown, all five partons are confined to the  $y-z$  plane so that the gluon polar angle covers the range  $0-2\pi$ . In each of the patterns shown, the gluon cross section shows sharp peaks in the vicinity of the  $b$  and  $\bar{b}$  quarks—the origin of the parton shower component of the  $b$ -jets. Also visible are very narrow holes coincident with the  $b$  and  $\bar{b}$  flight directions. These are known as “Dead Cones” and arise from the suppression of the collinear singularity due to the non-zero  $b$  quark mass. They also occur for the  $t$  and  $\bar{t}$  quarks. The angular extent of the dead cone is typically  $\sim 1/\beta$  and is thus much larger for the  $t$  or  $\bar{t}$  than for the much faster  $b$  or  $\bar{b}$ . In the presence of the top quark dead cones, the gluon emission cross section associated with a parton shower from the top quark is confined to low shoulders centered around the  $t$  and  $\bar{t}$  flight directions. Note that the description of this feature as being due “to the top quark” is not completely accurate since the radiation is from the color charge attached to both

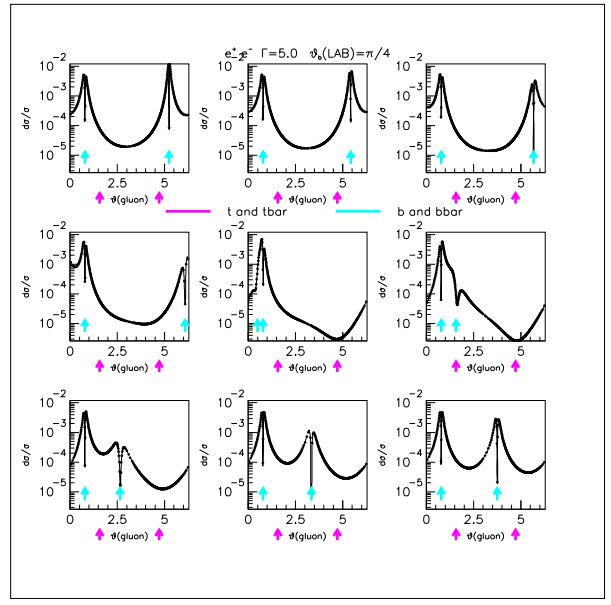


Figure 2: Radiation patterns calculated by eikonal description with the top width  $\Gamma_t = 5$  GeV. Each plot shows the single gluon production differential cross section (normalized to the hard scattering Born cross section) *vs* the polar angle  $\theta$ . Confined to two dimensions,  $0 < \theta < 2\pi$ .

the top and  $b$  quarks. The magnitude of this component is much smaller than that associated with the  $b$ -quarks, although the relative sizes are exaggerated in the patterns shown since the effects of coherence, that arise when multiple gluon emissions are included, are absent. As pointed out in Reference [?], the most probable kinematic configuration of the  $b$  and  $t$  or  $\bar{b}$  and  $\bar{t}$  is where they have similar flight directions so that it is very difficult to discern effects due to the presence of a showering top quark unless specific kinematic configurations can be chosen. One alternative that is similar in spirit and explored here is to study contributions to hadroproduction in the region of phase space isolated from reconstructed jets.

The coefficients in equation 1 are functions of  $\Gamma_t$ . Figure 2 shows the same radiation patterns as previous but with  $\Gamma_t = 5$  GeV. That the short lifetime effectively cuts off the soft radiation “from the top” is most clearly seen in those cases where the  $t$  or  $\bar{t}$  are separated from the  $b$  and  $\bar{b}$  so that different showers can be distinguished. In these cases, the  $t$  or  $\bar{t}$  showers which are visible for  $\Gamma_t = 0$  are gone when  $\Gamma_t = 5$  GeV. Experimental sensitivity to the lifetime will therefore need to focus attention on regions away from the  $b$  and  $\bar{b}$  quarks. The eikonal formalism also describes the dependence of the suppression due to

the finite width on the gluon energy; it is largest for the softest gluons. The gluon cross section is also proportional to  $d\omega/\omega$ , where  $\omega$  is the gluon energy, so that it is desirable to have sensitivity to the softest energy regimes. In Reference [?], the effects of gluons with energies of  $\omega = 5$  GeV were explored, in part as a consequence of the intent to study evidence for gluons in the form of extra soft jets. A better-matched technique would be to study the details of isolated hadrons, by using charged tracks for instance. By focusing on such properties as particle multiplicities, the experimentally problematic issue of resolving a gluon with energy  $\sim 1$  GeV as a jets is avoided. By using hadrons which are isolated, experimental efficiencies will be high. The kinematic properties of hadrons are also not an unreasonable means of understanding the disposition of the underlying partonic structure. Consequently, features such as the quark dead cones might be experimentally resolvable.

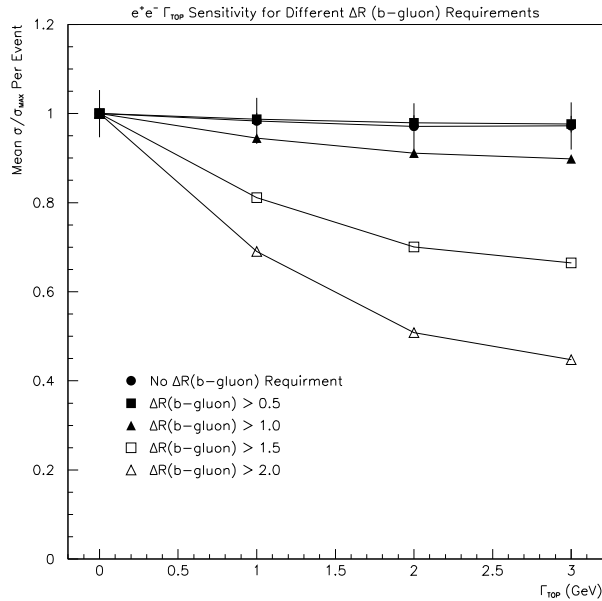


Figure 3: Suppression of the single gluon cross section as calculated by the eikonal description using kinematics folded in from the HERWIG Monte Carlo program. Each curve shows the effect for gluons with different isolation relative to the  $b$  and  $\bar{b}$  quarks in the events.

Because of the clear sensitivity of the radiation patterns to the kinematic configuration of the underlying partons, calculated expectations need to fold in a full description of events provided by a Monte Carlo program. Using such a program to sample phase space, the soft gluon production cross section can be cal-

culated for different kinematics which can then be subjected to experimental acceptances and other effects to estimate the suppression of the soft gluons under relatively realistic conditions. Figure 3 shows the suppression of the cross section for the production of a single gluon as a function of  $\Gamma_t$  assuming different isolation criteria imposed between the gluon and  $b$ -quarks emerging from the top quark decay. The result shows that if the soft isolated gluon multiplicity can be extracted from experimental measurements, the top quark width can be accordingly determined.

### 3.2 Parton Shower Models and Monte Carlo Programs

Many features of soft gluon emissions implied by the eikonal description are now contained in Monte Carlo programs such as HERWIG[?] and PYTHIA[?]. These Monte Carlos also contain the standard means for dealing with interference effects inherent in multi-gluon emissions as calculated from the Parton Shower model. While the production-decay stage interference effects are not included, such Monte Carlo programs provide the only reasonably accurate means of calculating expected experimental results particularly the unavoidable and dominant contributions from the fragmentation of  $b$ -quarks and decay of  $b$ -hadrons. The sought for interference effects are a small effect in comparison. In this context, features of gluon emission in  $t\bar{t}$  events as described by Monte Carlo programs are reviewed here. For  $e^+e^-$  collisions at  $\sqrt{s} = 500$  GeV, both Monte Carlos predict significant soft gluon production from the  $t$  and  $\bar{t}$ . The probability for at least one gluon is dictated by the Sudakov form factors which effectively resum leading log singularities and virtual corrections. The Sudakov form factors are expressed as functions of an ordering parameter which depends on the kinematics of the showering particle. In the case of the top quark, it is its low velocity that dictates values of Sudakov form factors which imply a low showering rate in the Parton Shower Model. Table 1 shows the rate and multiplicity of gluons for HERWIG and PYTHIA Monte Carlo programs at  $\sqrt{s} = 500$  GeV and  $\sqrt{s} = 1500$  GeV. The gluon emission rate in PYTHIA is slightly less than that in HERWIG although there is some sensitivity to the specific values for cutoff parameters that describe the boundary between the perturbative and non-perturbative regimes.

The energy distribution of the gluons described by the parton showers in Monte Carlo programs is dictated by the same cutoffs and by the  $1/\omega$  energy dependence of the single gluon cross section. HERWIG and PYTHIA of course use different param-

	HERWIG	PYTHIA	
$\sqrt{s}$	500 GeV	500 GeV	1500 GeV
$F_{rad}$	47.1	43.3	68.0
$\langle N_g \rangle$	1.9	1.0	1.0
$\langle N_g^{tot} \rangle$ (Dilepton)	8.58	5.8	8.33

Table 1: Average rate of production stage gluon emission from  $t$  or  $\bar{t}$  quarks in HERWIG and PYTHIA Monte Carlo programs.  $F_{rad}$  is the fraction of events for which there was at least one gluon emitted by a  $t$  or  $\bar{t}$  quark.  $\langle N_g \rangle$  is the average number of gluons emitted in  $t$  or  $\bar{t}$  parton showers, and  $\langle N_g^{tot} \rangle$  is the mean number of gluons from any source, quoted only for Dilepton events.

eters to specify the perturbative/non-perturbative threshold but typical values are always in the range 500 MeV – 1000 MeV. Figure 4 shows a variety of distributions obtained from the two programs describing the gluon energy. In any of the different guises, the typical energy of the gluons is  $\sim 2 - 3$  GeV with long tails.

For the results shown in this paper, the values of the two PYTHIA parameters,  $\Lambda_{QCD}$  and the shower cutoff  $Q_0$ , have been changed from their default ones to correspond more nearly to what is used in HERWIG.  $\Lambda_{QCD}$  is reduced from 250 MeV to 180 MeV. The cutoff  $Q_0$  was changed from 1 GeV to 1.7 GeV. This latter change gives the same effective gluon mass in the two programs and nearly the same quark masses. Parameters relevant to PYTHIA’s hadronization scheme ought to probably have been changed as well but were not. Clearly, a realistic scenario would require some tuning of these parameters on independent data samples.

The Monte Carlo programs also include the effect of non-zero masses on the kinematics of the emitted gluons. As previously discussed, the most visible effect of a finite mass is to suppress the collinear singularity. The implementation of the parton shower model in Monte Carlo programs is based on massless expressions (in the Altarelli-Parisi splitting functions for instance) and non-zero mass effects are imposed *ad hoc*. In HERWIG, a dead cone is introduced as a sharp step function in the emission probability as a function of the emitting object’s velocity [?]. PYTHIA matches the matrix element for single gluon emission to the parton shower result [?]. Figure 5 shows the radiation patterns for gluons from the two programs. The dead cone in PYTHIA is much less prominent than in HERWIG and might be more appropriately described as a “suppressed” cone than a “dead” cone.

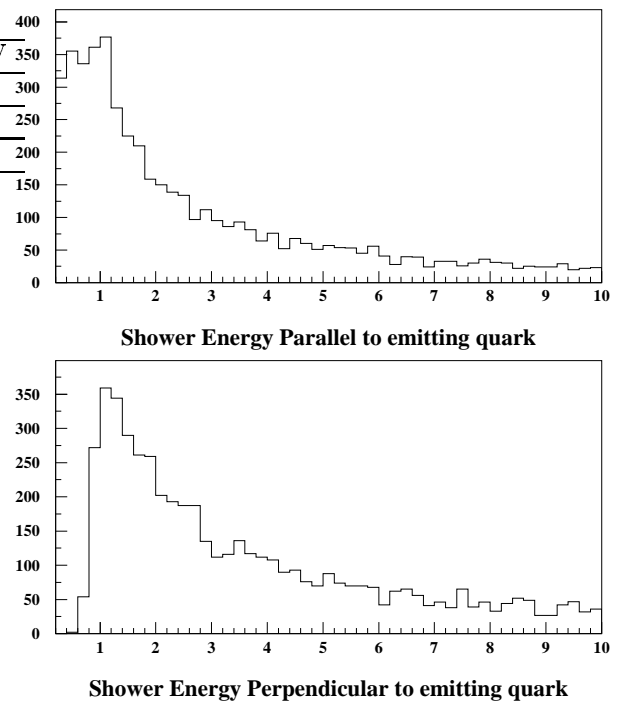


Figure 4: Energy characteristics of gluons emitted by top quarks in production from  $e^+e^-$  collisions.

## 4 Measurement of QCD Properties

Two measurements of interest that would be sensitive to the presence of top are the radiation pattern for hadrons measured as their angular distribution relative to reconstructed  $t/\bar{t}$  and the mean multiplicity of isolated hadrons. The former would be expected to carry information relevant to the dead cone pattern of gluons radiated from top and the latter would carry information about the multiplicity of gluons in the region of phase space which is more sensitive to the presence of top. A quantitative sketch of expectations for such measurements is presented here.

### 4.1 Measurement of Isolated Hadronic Radiation Pattern

The radiation pattern for hadrons can be defined as the distribution of  $dN/d\cos\theta$  where  $\theta$  is the angle between the hadron and the nearer of the reconstructed  $t$  or  $\bar{t}$ . To obtain sensitivity to the presence of a top quark, hadrons are required to be isolated from jets associated with the  $b$  and  $\bar{b}$  quarks and with any jets from hadronic  $W$  decays. The definition of  $\theta$  assumes that  $t$  and  $\bar{t}$  flight directions can be reconstructed. Constrained fit techniques to do this have

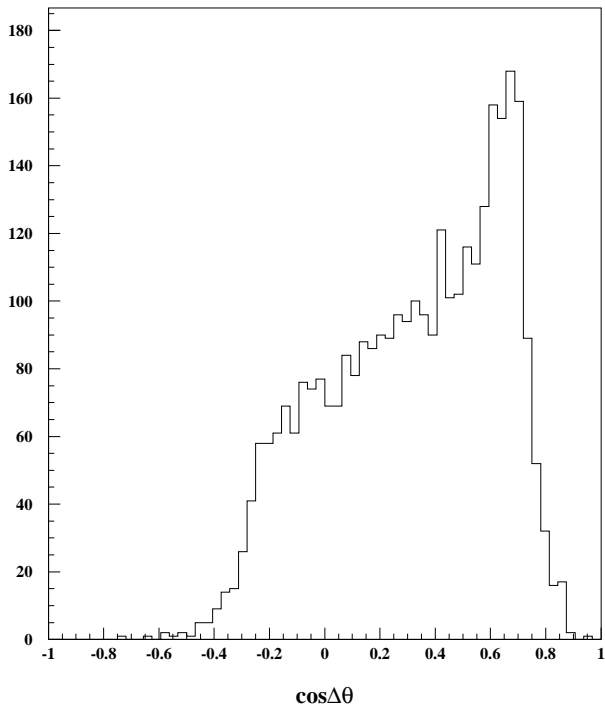


Figure 5: Radiation pattern calculated as the distribution  $\frac{dN}{d\cos\theta}$  for gluons emitted by top quarks using the HERWIG Monte Carlo program.

been used in experiments at the Tevatron [?] and it is assumed that similar or better results are achievable in a cleaner and more highly constrained linear collider environment. In lieu of a full detector simulation, the distributions shown are for stable hadrons rather than charged tracks which would presumably be used in a real measurement. Because of isolation requirements, track finding efficiencies should be high and the lack of a full simulation ought to have little effect on the results obtained.

Hadronic radiation patterns obtained from HERWIG are shown in Figure 7. Each pattern shows the  $\frac{dN}{d\cos\theta}$  distribution for stable hadrons sorted into “signal” and “background” categories according to whether they were nearer one of the partons from the  $t$  or  $\bar{t}$  electroweak decay or the leading gluon from any shower by the  $t$  or  $\bar{t}$ . As expected, there are many more background hadrons than signal hadrons. Also shown in Figure 7 is the effect on the two categories of imposing isolation and simple fiducial requirements ( $P_T > 1$  GeV/c,  $\cos\theta < 0.9$ , where  $\theta$  is the polar angle in the lab frame). One observes that the hadronic radiation pattern reasonably follows the gluon radiation patterns. Without the isolation requirements, the “background” multiplicity is much larger than the “signal” multiplicity. After requiring hadrons to be

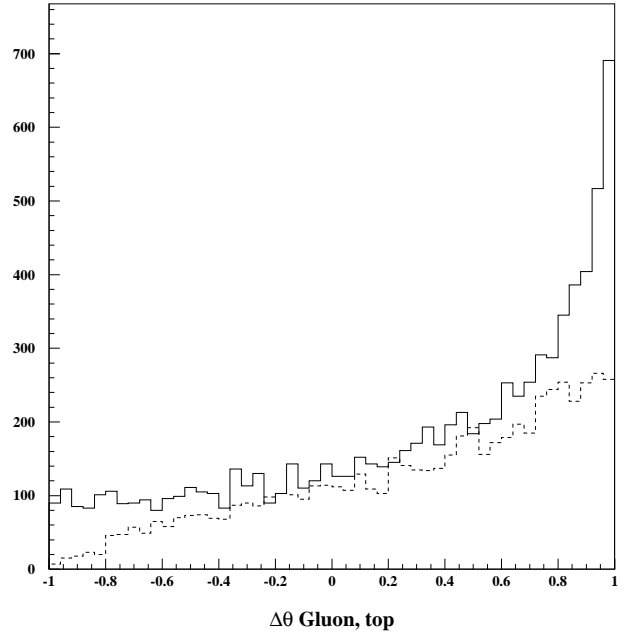


Figure 6: Radiation pattern for gluons emitted by top quarks as described by PYTHIA with (solid line) and without (dashed line) matrix element corrections.

isolated, the relative sizes are comparable. Fiducial requirements do not significantly change the shape or favor one category above the other. The presence of the two contributions ought to be discernible in a real experiment. One concern is that the hadrons in the “signal” category might really be due primarily to the “background” fragmentation shaped to look like signal by the circumstance of being near the gluon. This can be checked by: 1) Modifying the Monte Carlo program to suppress the production stage radiation from top; 2) Introduce a fictitious gluon with momentum vector relative to a top produced from the unmodified program; 3) clustering the resulting hadrons. The “signal” taken in this way ought to be an approximation of the background contribution to the signal distributions from Figure 7. Figure 8 shows the result compared to the unmodified results. Clearly the background contribution to the signal is only slightly sculpted by being near a gluon and the signal contribution is dominated by the effects of the hadrons produced in association from radiation by the  $t$  or  $\bar{t}$  quark.

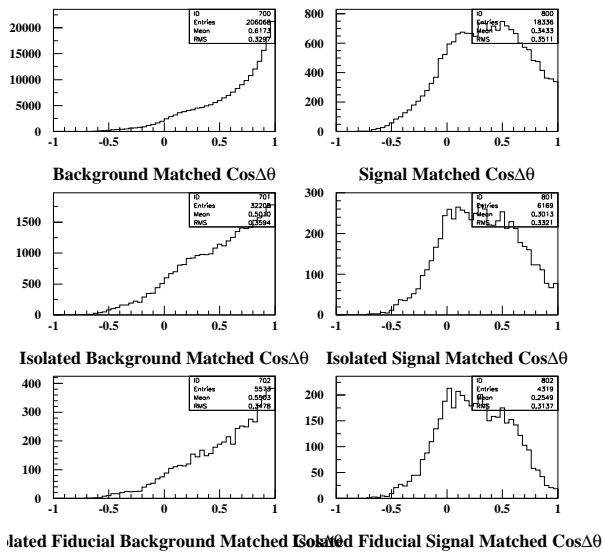


Figure 7: Hadron radiation patterns calculated by HERWIG Monte Carlo. Each plot shows the distribution  $\frac{dN}{d\theta}$  where  $\theta$  is the angle between each stable hadron and the nearer of the  $t$  or  $\bar{t}$  quark. Plots on the left hand side are for hadrons which are nearer the partons resulting from the  $t$  or  $\bar{t}$  electroweak decay than any radiated gluon while those on the right are for hadrons which are nearer to the lead gluon radiated from a  $t$  or  $\bar{t}$ . The upper two plots are for all hadrons, the middle two for hadrons which are required to be isolated from the electroweak partons, and the bottom two are for hadrons which are isolated and have  $P_T > 1$  GeV/c.

## 5 Mean Hadron Multiplicity and Measurement of $\Gamma_t$

Although the dependence of the single gluon emissions rate on the top lifetime has been extracted (*cf* Figure 3), the determination of  $\Gamma_t$  is complicated by the facts that 1) multiple gluon emission is the norm; and 2) gluons are not observable final states. The first problem will be addressed by focusing on those regions of phase space dominated by low gluon multiplicities. The second problem will be addressed in a necessarily model-dependent fashion by obtaining the correlation between gluon activity and the observed properties of hadrons as calculated by different Monte Carlo programs. In particular, the relationship calculated by Monte Carlo programs between the mean hadron multiplicity and the mean gluon multiplicity is explored.

In addition to the fundamental model dependence of describing hadroproduction, there are other diffi-

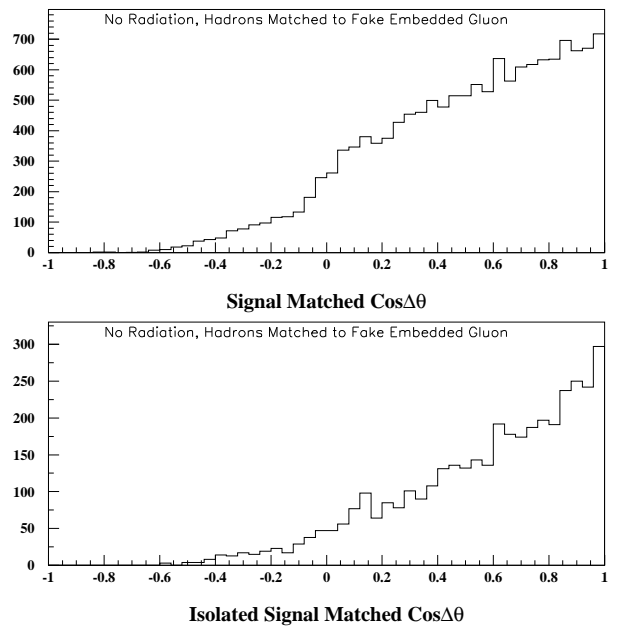


Figure 8: Radiation patterns calculated by eikonal description. Each plot shows the single gluon production differential cross section (normalized to the hard scattering Born cross section) *vs* the polar angle  $\theta$ . Confined to two dimensions,  $0 < \theta < 2\pi$ .

culties with correlating observed hadron properties with gluons. The origin of hadrons in an event is not as simple as the conversion of a gluon into some set of hadrons as would be the case in a decay. By way of example, consider the cluster picture of hadronization used in HERWIG. In this scheme, hadrons essentially emerge from the final state color segments, the number and kinematics of which are in turn driven by the particulars of gluon emission. One expects that the number of gluons would be correlated with the number of color segments (also referred to as clusters) and thence with the number of hadrons produced. This expectation can, however, break down. If, for example, one suppresses all emissions, then there are fewer color lines from which hadrons emerge but they also have a much higher mass than those present with gluon suppression enabled. In the HERWIG program, high mass clusters undergo division into smaller mass clusters until their mass is typical of that produced through the showering process so that in the end, the hadron multiplicity is not so different from the case where no emission is allowed. The role of the gluon emissions is effectively to place the hadrons in the right place rather than affect their rate. Without an isolation cut, the relationship between hadron and gluon multiplicity would be less clear and one would

also expect that for strong suppression of gluon emissions, the sensitivity to details of the hadronization model would be greatest.

Finally, one has to specify *which* gluons for which a correlation with observed hadrons is sought. Figure 9 shows the energy spectrum for gluons produced from parton showers in  $t\bar{t}$  event. The median energy is 2.6 GeV. One option is to use this value as a “typical” gluon and re-derive the curves in Figure 3; the curves shown were derived for 1 GeV gluons. Another option is to limit the derived correlation to the subset of gluons for which Figure 3 was derived. This is the approach taken here and is effected by correlating the mean gluon and hadron multiplicities using gluons with energies less than 3 GeV, or mean energies of  $\sim 1.2$  GeV. It should be understood that this does not mean that properties of the observed hadrons do not depend on the higher energy gluons.

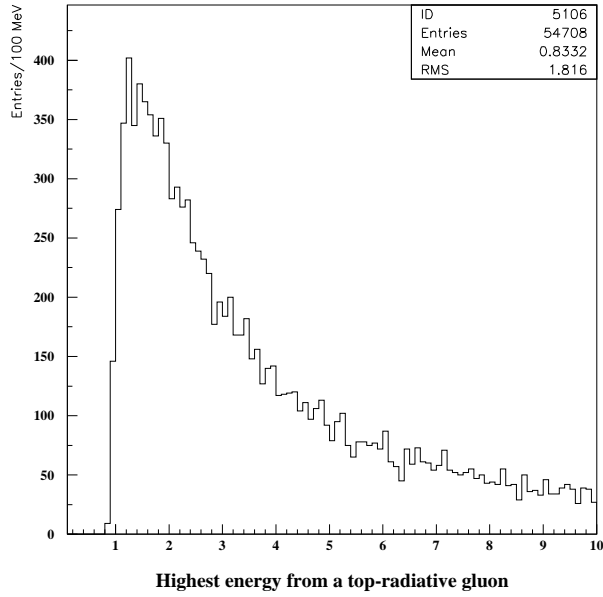


Figure 9: Energy spectrum of the hardest gluon emitted from top quarks obtained from HERWIG. The emission of a two or more gluons is much less probable than of a single gluon.

Figure 10 shows examples of the relationship obtained from HERWIG and PYTHIA between isolated hadron multiplicity and the number of isolated soft gluons produced. Such a plot can be used to derive the mean gluon multiplicity,  $N_g$ , given a measurement of the mean hadron multiplicity,  $N_h$ . As important, the statistical uncertainty in the hadron multiplicity can be easily determined and a corresponding uncertainty in the mean gluon multiplicity derived. From this value, the curves in Figure 3 then determine the

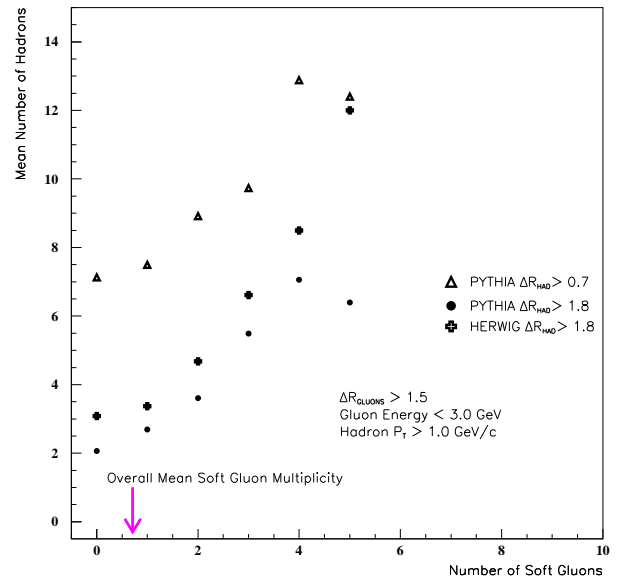


Figure 10: Dependence of isolated stable hadron multiplicity on isolated soft gluon multiplicity for HERWIG and PYTHIA Monte Carlo programs.

precision with which  $\Gamma_t$  is extracted.

It is of interest to compare the sensitivity for the determination of  $N_g$  using different isolation criteria required of the hadrons. In addition to focusing attention on regions of phase space that are more sensitive to effects of showers from the top quarks, the isolation criterion can also affect the contributions to the hadron multiplicities that arise from sources other than parton showers. Figure 10 shows that even for the case of no gluons, some hadrons are always present. A large source of such hadrons are due to decays of  $B$  hadrons which are the leading source of hadrons near the jet core. Clearly, the precision with which  $N_g$  is derived should improve with a tightened isolation criterion that removes this contribution. Figure 11 shows the precision obtained on  $N_g$  as a function of  $\Delta R$ , the isolation of hadrons with respect to the hard jets, for samples of 10,000 events;  $\Delta R$  is defined as  $\sqrt{\Delta\eta^2 + \Delta\phi^2}$ , where  $\eta$  is the pseudo-rapidity and  $\phi$  is the azimuthal angle.

The precision is calculated for Dilepton and Lepton+Jet decays and for gluons with isolation of  $\Delta R > 1.0$  and  $\Delta R > 1.5$ . Of course, one cannot determine whether a given event has had gluons with the given isolation and the evaluation of  $N_g$  separately for two categories (*i.e.* those gluon  $\Delta R > 1.0$  and  $> 1.5$ ) is simply a calculational artifice that emphasizes the phase space from which most of the information is obtained. One could separately use the relationship between hadron multiplicity and, say, gluons with iso-

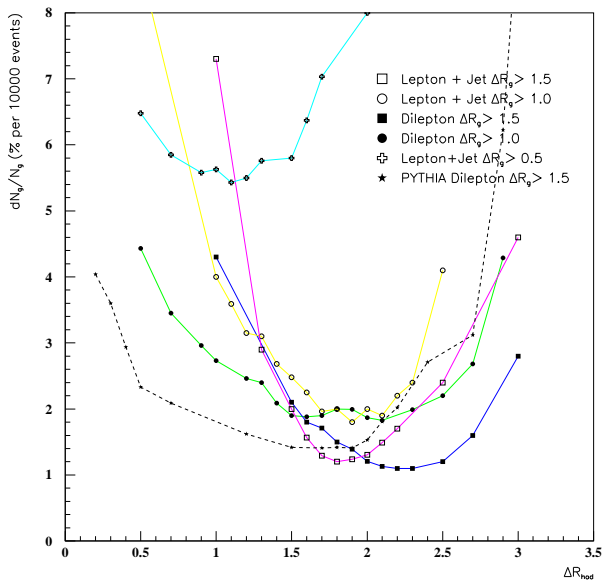


Figure 11: Statistical precision with which the isolated soft gluon multiplicity is inferred from the measurement of the isolated hadron multiplicity for 10000 events of different decay modes.

lations  $\Delta R < 1.0$ ,  $1.0 < \Delta R < 1.5$ , and  $\Delta R > 1.5$  and then average the results but the result will be dominated by the results of the last category. For a different hadron isolation, the relevant region of phase space would be different. The curves shown in Figure 11 show that for a particular hadron isolation, there is a subset of gluons for which the measured multiplicity can be most precisely determined and, as one might have suspected, they are the gluons that have similar isolation characteristics as the chosen hadrons.

By combining the the previously described relationship between the gluon cross section and  $\Gamma_t$  shown in Figure 3 with the curves in Figure 11, the precision with which  $\Gamma_t$  is extracted from the mean isolated hadron multiplicity can be evaluated. After correcting for the branching ratios, the best precision is obtained for the Lepton+Jet decay mode and hadron isolation  $\Delta R > 1.5$ . Under those conditions, 10,000 events, or approximately 1-2 years of running at design luminosities for  $\sqrt{s} = 500$  GeV, would give a 2% statistical measurement on  $\Gamma_t$ .

## 6 Conclusion

The study of hadroproduction offers a method to study the properties of soft gluons in events. Perturbative QCD predicts distinctive and testable features of hadrons originating from showers due to massive

colored objects. In particular, evidence for jettiness of top quarks with a suppressed core due to the suppression of the mass singularity should be evident in the distribution of opening angles between hadrons and reconstructed top flight directions. The measurement of the mean isolated hadron multiplicity appears to have a sensitivity which would yield a measurement of  $\Gamma_t$  to an uncertainty of a few percent which would be competitive with measurements of the line shape at threshold. An important limitation would be the momentum acceptance of a tracking chamber.